

Global response of terrestrial ecosystem structure and function to CO2 and climate change: results from six dynamic global vegetation models

Wolfgang Cramer, Alberte Bondeau, F. Ian Woodward, I. Colin Prentice, Richard Betts, Victor Brovkin, Peter Cox, Veronica Fisher, Jonathan Foley, Andrew Friend, et al.

▶ **To cite this version:**

Wolfgang Cramer, Alberte Bondeau, F. Ian Woodward, I. Colin Prentice, Richard Betts, et al.. Global response of terrestrial ecosystem structure and function to CO2 and climate change: results from six dynamic global vegetation models. Global Change Biology, 2001, 7 (4), pp.357-373. 10.1046/j.1365-2486.2001.00383.x . hal-01757651

HAL Id: hal-01757651
https://hal.science/hal-01757651

Submitted on 14 Sep 2022

HAL is a multi-disciplinary open access archive for the deposit and dissemination of scientific research documents, whether they are published or not. The documents may come from teaching and research institutions in France or abroad, or from public or private research centers.

L'archive ouverte pluridisciplinaire **HAL**, est destinée au dépôt et à la diffusion de documents scientifiques de niveau recherche, publiés ou non, émanant des établissements d'enseignement et de recherche français ou étrangers, des laboratoires publics ou privés.



Distributed under a Creative Commons Attribution - NonCommercial 4.0 International License

Global response of terrestrial ecosystem structure and function to CO_2 and climate change: results from six dynamic global vegetation models

Wolfgang Cramer[1], Alberte Bondeau[1], F. Ian Woodward[2], I. Colin Prentice[3], Richard Betts[4], Victor Brovkin[2], Peter Cox[4], Veronica Fisher[5], Jonathan Foley[5], Andrew Friend[6], Chris Kucharik5, Mark Lomas[2], Navin Ramankutty[5], Stephen Sitch[1], Benjamin Smith[7], Andrew White[6], Christine Young-Molling[5]

[1]*Potsdam Institut für Klimafolgenforschung (PIK) e.V., Telegrafenberg, PO Box 60 12 03, D-144 12 Potsdam, Germany,*
[2]*Department of Animal & Plant Sciences, University of Sheffield, Sheffield S10 2TN, UK,*
[3]*Max-Planck-Institut für Biogeochemie, PO Box 100164, D-07701 Jena, Germany,*
[4]*Hadley Centre for Climate Prediction and Research, Meteorological Office, Bracknell, Berkshire RG12 2SY, UK,*
[5]*Institute for Environmental Studies, University of Wisconsin-Madison, Madison, WI 53706, USA,*
[6]*Institute of Terrestrial Ecology, Bush Estate, Penicuik EH26 0QB, UK,*
[7]*Climate Impacts Group, Department of Ecology, University of Lund, Ekologihuset, S-223 62 Lund, Sweden*

The possible responses of ecosystem processes to rising atmospheric CO2 concentration and climate change are illustrated using six dynamic global vegetation models that explicitly represent the interactions of ecosystem carbon and water exchanges with vegetation dynamics. The models are driven by the IPCC IS92a scenario of rising CO2 (Wigley et al. 1991), and by climate changes resulting from effective CO2 concentrations corresponding to IS92a, simulated by the coupled ocean atmosphere model HadCM2-SUL. Simulations with changing CO2 alone show a widely distributed terrestrial carbon sink of 1.4–3.8 Pg C y−1 during the 1990s, rising to 3.7–8.6 Pg C y−1 a century later. Simulations including climate change show a reduced sink both today (0.6–3.0 Pg C y−1) and a century later (0.3–6.6 Pg C y−1) as a result of the impacts of climate change on NEP of tropical and southern hemisphere ecosystems. In all models, the rate of increase of NEP begins to level off around 2030 as a consequence of the 'diminishing return' of physiological CO2 effects at high CO2 concentrations. Four out of the six models show a further, climate-induced decline in NEP resulting from increased heterotrophic respiration and declining tropical NPP after 2050. Changes in vegetation structure influence the magnitude and spatial pattern of the carbon sink and, in combination with changing climate, also freshwater availability (runoff). It is shown that these changes, once set in motion, would continue to evolve for at least a century even if atmospheric CO2 concentration and climate could be instantaneously stabilized. The results should be considered illustrative in the sense that the choice of CO2 concentration scenario was arbitrary and only one climate model scenario was used. However, the results serve to indicate a range of possible biospheric responses to CO2 and climate change. They reveal major uncertainties about the response of NEP to climate change resulting, primarily, from differences in the way that modelled global NPP

Correspondence: Wolfgang Cramer, Fax: + 49 331288 2600, E-mail: Wolfgang.Cramer@pik-potsdam.de
[1]Present adress: Center for Environmental Prediction, Rutgers University, 14 College Farm Road, New Brunswick, NJ 08901–8551, USA, at NASA Goddard Institute for Space Studies, 2880 Broadway, New York, NY 10025, USA
[2]Present address: Department of Mathematics, Heriot-Watt University, Edinburgh EH14 4AS, UK

responds to a changing climate. The simulations illustrate, however, that the magnitude of possible biospheric influences on the carbon balance requires that this factor is taken into account for future scenarios of atmospheric CO2 and climate change.

Keywords: dynamic global vegetation model, global carbon cycle

Introduction

Recognizing the importance of land ecosystems in the global carbon cycle, the Kyoto Protocol to United Nations Framework Convention on Climate Change (1997) recommends the protection, enhancement and quantification of terrestrial biospheric sinks for anthropogenic CO_2 emissions. During the 1980s, oceanic and terrestrial uptake of CO_2 each amounted to a quarter to a third of anthropogenic CO_2 emissions but with strong interannual variability (Braswell *et al*. 1997; Prentice *et al*. 2000) and uncertainty about the major location of the terrestrial sink (Dixon *et al*. 1994; Ciais *et al*. 1995; Keeling *et al*. 1995; Keeling *et al*. 1996a; Keeling *et al*. 1996b; Lloyd & Farquhar 1996; Fan *et al*. 1998; Heimann & Kaminski 1999; Houghton *et al*. 1999; Rayner *et al*. 1999). Terrestrial ecosystems are thus a critical component of the global carbon cycle; requiring a better understanding of their decadal to century-scale carbon balance dynamics, both for interpreting observed variations in atmosphere-biosphere carbon exchanges (Fung *et al*. 1997) and for evaluating policies to mitigate anthropogenic CO_2 emissions (United Nations Framework Convention on Climate Change 1997; IGBP Terrestrial Carbon Working Group 1998).

Terrestrial biogeochemical models, forced by transient scenarios of increasing atmospheric CO_2 concentration and associated changes in climate, but assuming a constant distribution of vegetation, have indicated that the terrestrial carbon sink, as far as it is generated by increasing CO_2, still has the potential to increase but cannot persist indefinitely at high strength (King *et al*. 1997; Cao & Woodward 1998). The eventual decline shown in these simulations has two main causes: on the one hand, the direct physiological effects of CO_2 on productivity and water-use efficiency decrease with increasing CO_2 concentration, approaching an asymptote at high CO_2 concentrations. On the other hand, heterotrophic respiration increases with temperature so that global warming scenarios generally lead to reduced terrestrial carbon uptake, compared with what would be expected if climate remained constant.

Such models cannot consider the consequences of climate-induced changes in vegetation *structure* on the terrestrial carbon sink, although some early calculations have suggested that vegetation change, with climatic warming, might cause a significant carbon release (Neilson 1993; Smith & Shugart 1993), as well as other changes in ecosystem services. Equilibrium biogeography models that do simulate changes in vegetation composition and structure have also been used for assessments of climate impacts on ecosystems, for example in VEMAP Members (1995), Cramer (1996) and in recent IPCC reports (Watson *et al*. 1996; Neilson *et al*. 1998). All of these assessments show that we should expect significant vegetation changes as a result of anthropogenic changes in climate. However, equilibrium models do not simulate the processes of plant growth, competition, mortality, and changes in ecosystem structure that govern the dynamics of vegetation change. Transient changes in vegetation structure, in turn, can affect CO_2 and water exchange between the land and atmosphere.

Projecting transient terrestrial ecosystem responses under rapid climate change thus requires more comprehensive models that include vegetation dynamics, as well as biogeochemical processes. Dynamic global vegetation models (DGVMs) have been developed, primarily to fulfil this need (Prentice *et al*. 1989; Steffen *et al*. 1992). Here we present parallel results using six DGVMs, with differing levels of complexity and emphasis on different functionalities. The DGVMs and their principal investigators are HYBRID (Friend *et al*. 1997), IBIS (Foley *et al*. 1996), LPJ (Haxeltine & Prentice 1996a; Sitch 2000), SDGVM (Woodward *et al*. 1998; Woodward *et al*., in press), TRIFFID (P. Cox, pers. comm.), VECODE (Brovkin *et al*. 1997). Each model simulates linked changes in ecosystem function (water, energy and carbon exchange) and vegetation structure (distribution, physiognomy) in response to a common scenario of changes in CO_2 concentration and climate obtained with the coupled atmosphere–ocean general circulation model HadCM2-SUL (Mitchell *et al*. 1995; Johns *et al*. 1997). The results illustrate the range of responses of state-of-the-art terrestrial biosphere models to one particular scenario of atmospheric composition and climate change. We focus on the common features of the response shown by most or all models, as well as on significant variations between models that represent a potential source of uncertainty. Such uncertainties arise mainly about the

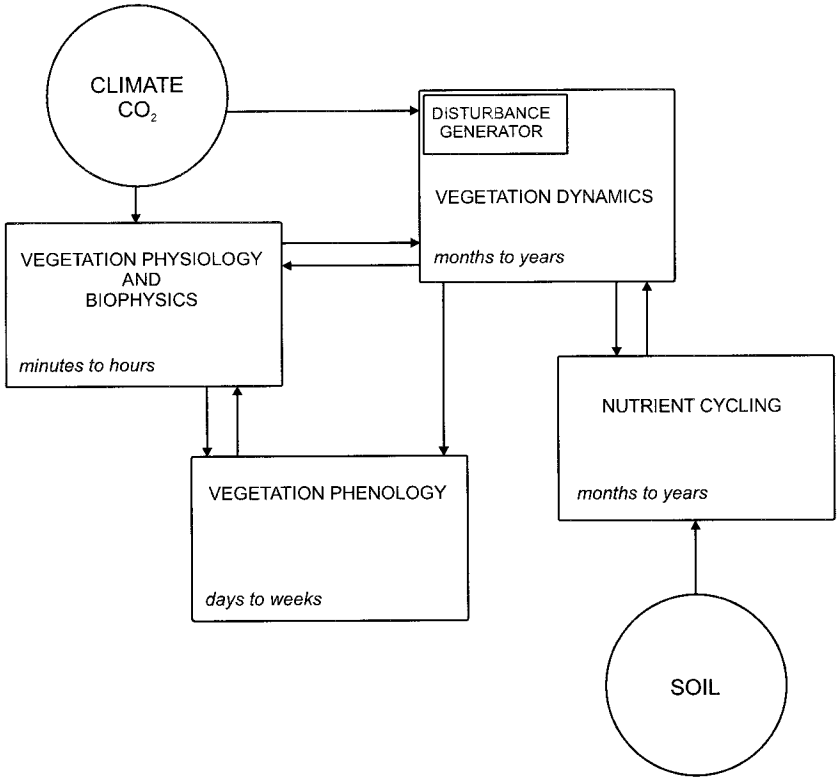


Fig. 1 Modular structure of a generic dynamic global vegetation model (DGVM) as employed with various modifications by the six models. The time steps of the modules are shown in italics.

response of the terrestrial carbon balance, in addition to the uncertainty due to differences in the predictions of climate models.

Methods and data

DGVM structure: overview

The representation of physiological, biophysical and biogeochemical processes in DGVMs (Fig. 1, Table 1) include more or less mechanistic representations of photosynthesis, respiration and canopy energy balance, the controls of stomatal conductance and canopy boundary-layer conductance, and the allocation of carbon and nitrogen within the plant. In two of the models (HYBRID and SDGVM), particular emphasis is given to the detailed description of plant physiological processes, including carbon–nitrogen interactions. Three other models (IBIS, TRIFFID and VECODE) are designed directly for inclusion in coupled atmosphere–biosphere models; they, too, use physiological formulations (IBIS with much greater detail than TRIFFID and VECODE), but are directly adapted for simulating the energy and water fluxes needed by the atmospheric general circulation model (or, in the case of VECODE, the intermediate complexity Earth System model CLIMBER2, Ganopolski *et al*. 1998). LPJ is designed primarily as a vegetation dynamics model with explicit scaling of individual-level processes to the grid cell, employing biophysical and physiological process parameterizations as in the equilibrium model BIOME3 (Haxeltine & Prentice 1996a). All DGVMs treat vegetation cover as a fractional representation consisting of different types.

Canopy phenology includes the seasonal timing of budburst, senescence and leaf abscission in response to temperature and/or drought. Vegetation dynamics are based on annual net primary production and biomass growth; they include competition among plant functional types, probabilities of natural disturbance (fire, general mortality) and succession (replacement of plant functional types over time) following disturbance. These processes are simulated either explicitly (e.g. in SDGVM and LPJ) or implicitly (e.g. in TRIFFID and VECODE). Some of the accumulated biomass in vegetation falls on to the ground as litter. The fate of this litter, and of cohorts from previous years, is subsumed under decomposition/nutrient cycling, which includes soil respiration and the net mineralization of nitrogen for uptake by plants. Soil hydrology depends on the (prescribed) soil texture and vegetation biophysical processes and

Table 1 Process descriptions in participating Dynamic Global Vegetation Models

	HYBRID	IBIS	LPJ	SDGVM	TRIFFID	VECODE
Shortest time step	12 h	1 h	1 d	1 d	2 h	1 yr
Physiology						
Photosynthesis	Farquhar *et al.* (1980)	Farquhar *et al.* (1980)/ Collatz *et al.* (1992)	Farquhar *et al.* (1980)/ Collatz *et al.* (1992)	Farquhar *et al.* (1980)/ Collatz *et al.* (1992)	Collatz *et al.* (1991)/ Collatz *et al.* (1992)	empirical NPP estimation (modified Lieth formula)
Stomatal conductance	Jarvis (1976)/Stewart (1988)	Leuning (1995)	Haxeltine & Prentice (1996b)	Leuning (1995)	Cox *et al.* (1998);	"
Canopy scaling	Optimum N_{leaf} distribution	Optimum N_{leaf} distribution	Optimum N_{leaf} distribution	Optimum N_{leaf} distribution	Optimum N_{leaf} distribution Sellers *et al.* 1992	"
Sapwood respiration	Dependent on sapwood volume and temperature	Diagnose sapwood volume from evaporative demand + LAI	Dependent on sapwood mass and C:N ratio (Lloyd & Taylor 1994)	Annual sapwood increment, C:N f(T)	Pipe model to diagnose sapwood volume, then Q_{10} relationship	"
Fine root respiration	f(T, N_{root})	f(T, C_{root})	f(T, C_{root})	f(T, C_{root})	f(T, N_{root})	"
Evapotranspiration	Penman–Monteith transpiration (Monteith & Unsworth 1990) + interception + evaporation from soil surface	Based on vapour pressure deficit and stomatal conductance (Pollard & Thompson 1995)	total evapotranspiration (Monteith 1995)	Penman – Monteith transpiration (Monteith 1981) + interception + evaporation from soil surface	Penman – Monteith transpiration (Monteith 1981) + interception (Fixed fraction)	n/a
Water balance	3 soil layers Darcy's law Drainage Snowpack (dynamic water holding capacity)	6/12 soil layers Darcy's law Surface runoff + drainage 3-layer snow model Soil T, soil q, soil ice	2 soil layers Modified bucket model from Neilson (1993) Surface runoff + drainage Snowpack	3 soil + 1 litter layer Modif. Bucket model Drainage Snowpack	1 soil layer Darcy's law	n/a
Canopy temperature	Canopy energy balance (Friend 1995)	Canopy energy balance (Pollard & Thompson 1995)	n/a	n/a	Diagnosed from energy balance	n/a
Aerodynamics	n/a	log – wind profile + momentum diffusion	n/a	log – wind profile	Neutral transfer coefficients using z_0 proportional to height	n/a
Radiation	Beer's Law (applied to individuals) visible + near IR	Two stream approximation (Sellers 1985; Pollard & Thompson 1995)	Beer's Law (applied to vegetation fractions)	Beer's Law (applied to total vegetation)	Beer's Law (applied to vegetation fractions)	n/a
Ecosystem structure						
Phenology						
Cold deciduous	GDD requirement daylength	Temperature threshold (can be modified by chilling)	GDD requirement Temperature threshold	Temperature threshold	Temperature sum with threshold	n/a
Dry deciduous	Soil moisture threshold	Productivity threshold	Soil moisture threshold	Soil moisture threshold	n/a	n/a
Grass	Carbon balance threshold	Productivity threshold	Soil moisture and temperature thresholds	Growth threshold	n/a	n/a
Litter fall	Daily litter carbon balance	Annual litter carbon balance	Annual litter carbon balance	Annual litter carbon balance	Monthly litter	Annual litter carbon balance
Decomposition	CENTURY (Parton *et al.* 1993), modified by Comins & McMurtrie (1993)	f (T, θ_{top}, tissue type)	f (T, θ_{top}, tissue type)	Similar to CENTURY (Parton *et al.* 1993)	f(T, θ, C_{soil}) McGuire *et al.* (1992)	f (T, tissue type)

		HYBRID	IBIS	LPJ	SDGVM	TRIFFID	VECODE
C allocation		Annual based on foliage	Annual with fixed allocation coefficients for leaves, stems, roots	Annual allometric relationships for individuals	Annual allocation by demand in order of priority LAI > roots > wood	Partitioning into 'spreading' and 'growth' based on LAI leaf:root:wood partitioning from allometric relationships	Annual with climate dependent allocation coefficients for 'green' and 'non-green' phytomass
N uptake		Function of soil mineral N, fine root mass, temperature and plant C:N ratio	n/a	n/a	Based on soil C and N decomposition also dependent on soil T and moisture	n/a	n/a
N allocation		Fixed C: N	n/a	Implicit, dependent on demand	Fixed C: N	Fixed C:N	n/a
pfts							
Trees	Evergreen	Broadleaf evergreen	Tropical evergreen Temperate evergreen	Tropical evergreen Temperate broadleaf evergreen	Broadleaf evergreen	Broadleaf	Evergreen trees
		Needleleaf evergreen	Cool conifer Boreal conifer	Temperate needleleaf evergreen Boreal needleleaf evergreen	Needleleaf evergreen	Needleleaf	
	Deciduous	Broadleaf dry deciduous Broadleaf cold deciduous Needleleaf dry deciduous Needleleaf cold deciduous	Tropical raingreen Temperate summergreen Boreal summergreen	Tropical raingreen Temperate summergreen Boreal summergreen	Broadleaf deciduous Needleleaf deciduous		Deciduous trees
Shrubs		n/a	n/a	n/a	Shrubs	Shrubs	n/a
Grasses/forbs		C3 herbaceous C4 herbaceous	C3 herbaceous C4 herbaceous	C3 herbaceous C4 herbaceous	C3 herbaceous C4 herbaceous	C3 herbaceous C4 herbaceous	Herbaceous
Vegetation dynamics							
Competition		Individual-based competition for light, N, H_2O within 'patches'	Homogenous area-based competition for light (2 layers), H_2O (6 layers)	Nonhomogenous area-based competition for light (1 layer), H_2O (2 layers)	Nonhomogenous area-based competition for light (1 layer), H_2O (3 layers)	Lotka–Volterra in fractional cover	Climate-dependent
Establishment		All PFTs establish uniformly as small individuals	Climatically favoured PFTs establish uniformly, as small LAI increment	Climatically favoured PFTs establish in proportion to area available, as small individuals	climatically favoured PFTs establish in proportion to area available, as small individuals	Minimum 'seed' fraction for all pfts	n/a
Mortality		Dependent on carbon pools	Deterministic baseline wind throw fire extreme temperatures	Deterministic baseline self-thinning carbon balance fire extreme temperatures	Carbon balance wind throw fire extreme temperatures	Prescribed disturbance rate for each pft	Climate-dependent, based on carbon balance

Abbreviations: N_{leaf}, leaf nitrogen concentration; N_{root}, root nitrogen concentration; T, temperature; θ,soil water content; z_0, roughness length.

influences both plant (physiology, phenology) and soil (soil respiration, nitrogen mineralization) behaviour. Again the degree of complexity in the representation of these processes varies among models.

Details about the different model formulations can be found in Table 1 and the original model publications. The table indicates the breakdown into 'plant functional types' (PFTs) that each model uses. PFTs are central to DGVMs because, on the one hand, they are assigned different parameterizations with respect to ecosystem processes (e.g. phenology, leaf thickness, minimum stomatal conductance, photosynthetic pathway, allocation, rooting depth), while on the other, the proportional representation of different PFTs at any point in time and space defines the structural characteristics of the vegetation (Woodward & Cramer 1996; Cramer 1997).

There is no spatially explicit treatment of propagule dispersal in these models, because several lines of reasoning suggest that migration of dominant plant species involves not only dispersal but also the development of mature individuals producing propagules. This development implies additional delays resulting from growth and competition processes (Pitelka & Plant Migration Workshop Group 1997; Clark *et al*. 1998). The results presented here consider stand development, but no dispersal. They therefore confirm that these processes may cause lags of a century or more in the response of vegetation to climate change.

Experimental design

All DGVM runs for this study were initialized with bare ground, of defined uniform soil texture, and run to equilibrium in a constant, pre-industrial CO_2 concentration and climate. The resulting simulated distributions of potential natural vegetation, summarized as biomass and leaf area index (LAI) values for the aggregated PFTs grass (C3 plus C4), deciduous trees and evergreen trees, were compared to a simplified map of natural vegetation inferred from NOAA-AVHRR satellite imagery (Fig. 2). The map was derived from the DISCover dataset (Loveland & Belward 1997) using an empirical algorithm to exclude crops and identify natural vegetation based on the most commonly occurring nonagricultural vegetation type in each grid cell.

For computational economy, the DGVMs were run at the same grid resolution as the climate model (3.75° longitude × 2.5° latitude, in total 1631 land grid cells). They were run 'off-line', i.e. biogeophysical and biogeochemical feedbacks from biospheric changes to climate and CO_2 concentration (Melillo *et al*. 1996; Sellers *et al*. 1996; Betts *et al*. 1997; Prentice *et al*., 2000) were not included. Changes in anthropogenic nitrogen deposition were neglected in all models except HYBRID. The impacts of increased nitrogen deposition, associated with industrial and agricultural activity, are potentially important to the carbon cycle through changes in plant nutrient availability (Schimel 1998; Nadelhoffer *et al*. 1999), and it will also be important to account for the negative impacts of parallel changes in tropospheric ozone. However, these effects are not yet included in DGVMs. The simulations thus take into account *only* the impacts of changing CO_2 and climate on natural or seminatural ecosystems. Incorporation of land use and inclusion of effects of atmospheric chemistry changes other than CO_2 are tasks for the future.

Three experiments were performed with each model: (i) changing CO_2 and constant, preindustrial climate (C); (ii) Hadley Centre climate model projections of CO_2-induced climate change and a constant, preindustrial CO_2 concentration (T); (iii) changes in both climate and CO_2 (CT). For experiment T, the climate model output for 1861–2099 was applied while the DGVMs were held to a fixed pre-industrial concentration of CO_2. For experiment C, the simulated pre-industrial climate was applied repetitively throughout the experiment while the DGVMs were allowed to respond to increasing CO_2 concentrations defined by IS92a. Experiment CT combined the forcings from the other two experiments. A final 100-y period with no further change in CO_2 or climate was appended to the end of each simulation, in order to investigate possible lags in the responses of ecosystems to changes in CO_2 and climate.

Climate and CO_2 scenarios

The time series of climate from 1861 to 2100 was derived from a simulation by the Hadley Centre climate model HadCM2-SUL (Mitchell *et al*. 1995; Johns *et al*. 1997) forced by observations and projections of sulphate aerosols and CO_2 corresponding to the IS92a IPCC scenario (Houghton *et al*. 1992). The time series of simulated surface air temperature change since 1860 (Fig. 3) compares well with observed change at spatial scales of 5000 km and above (Jones 1994; Mitchell *et al*. 1995; Johns *et al*. 1997) and the frequency and amplitude of the global and zonal mean annual variability (crucial for DGVMs) are also well reproduced (Tett *et al*. 1997). The simulated patterns of precipitation capture the observed zonal mean variations in the sensitivity of precipitation to surface warming (Hulme *et al*. 1998).

The sensitivity of HadCM2 to a doubling of CO_2 falls in the middle of the range of sensitivities of other GCMs of this generation (Kattenberg *et al*. 1996). Thus, we consider this climate change scenario representative of current attempts to model the climate response to IS92a. However, the spatial pattern of changing climate differs between GCMs (Watson *et al*. 1998), therefore the

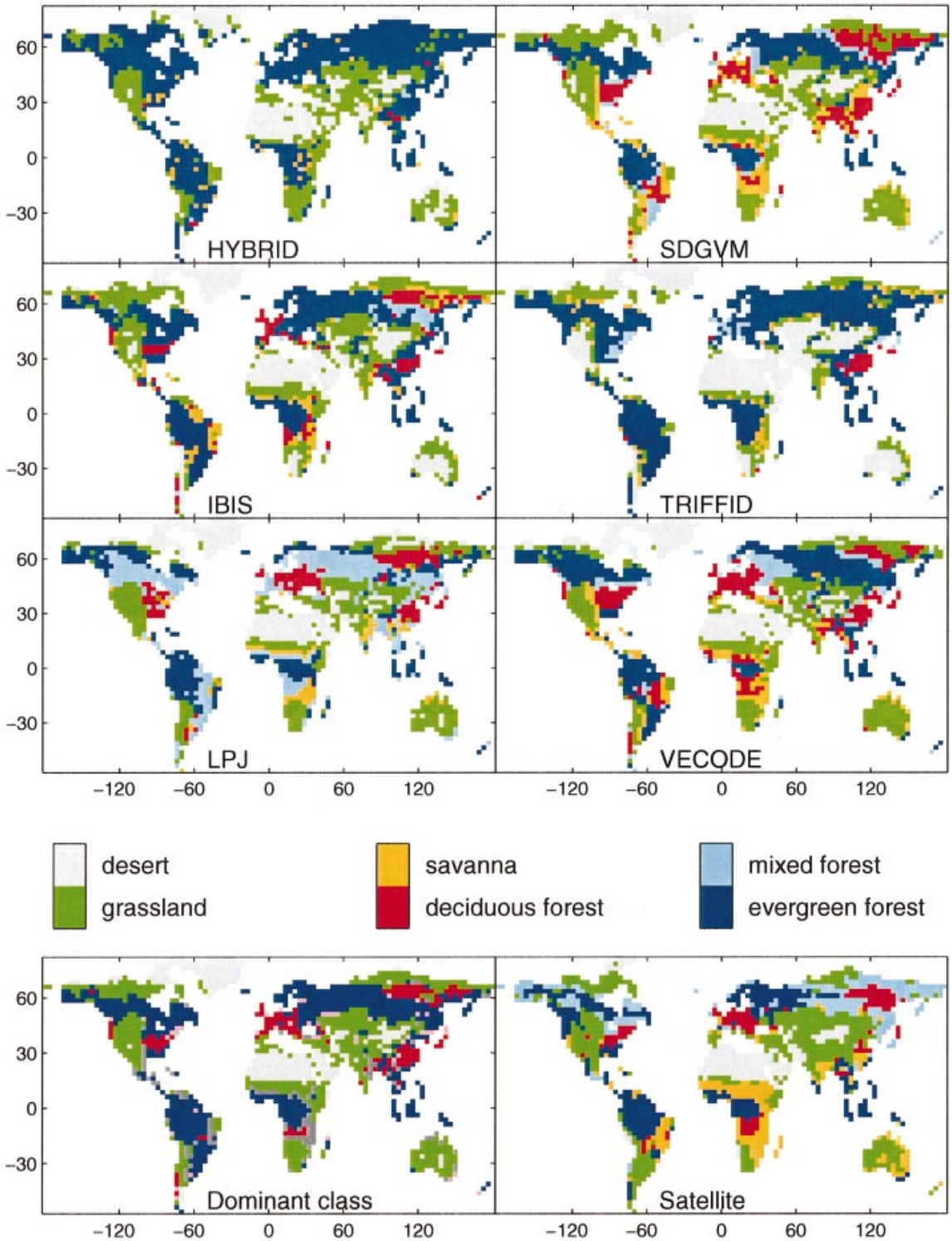


Fig. 2 Potential natural vegetation simulated by six DGVMs. The 'dominant class' in the bottom left panel is the vegetation class modelled by the largest number of models in each grid cell. The bottom right panel is a simplified map of natural vegetation inferred from NOAA-AVHRR satellite imagery, derived from the DISCover data set (Loveland & Belward 1997) using an empirical algorithm to exclude crops and identify natural vegetation based on the most commonly occurring nonagricultural vegetation type in each grid cell (Navin Ramankutty, pers. comm.).

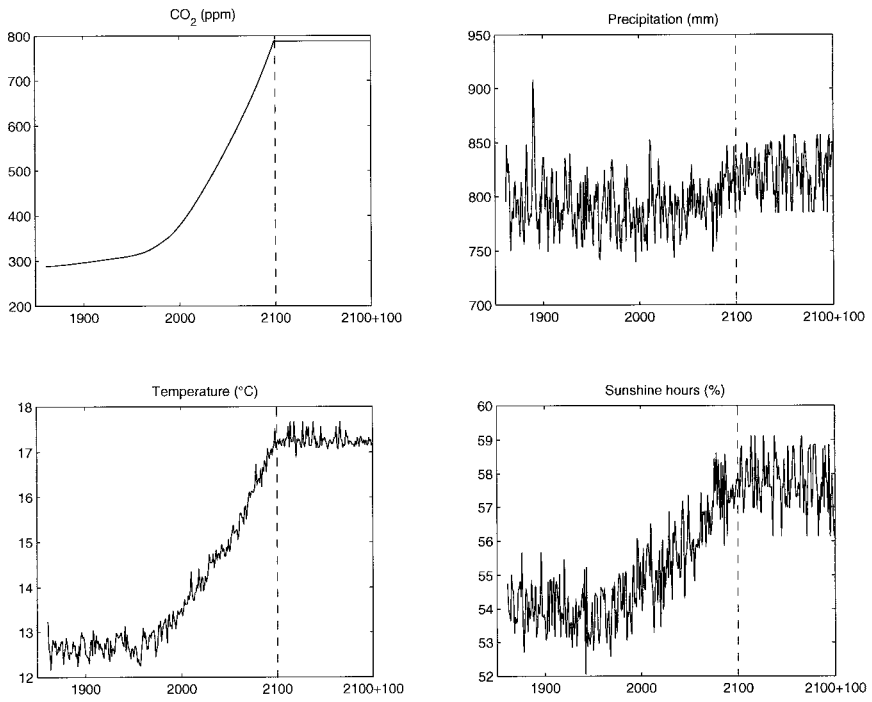


Fig. 3 IPCC IS92a projections of atmospheric CO_2 concentration and the HadCM2 SUL climate model simulations of temperature, precipitation and percentage sunshine over land (excluding Antarctica). CO_2 and mean climate are held constant after 2100 (dashed line).

regional-scale patterns of the scenario used here must be considered specific to that model.

All experiments were made using monthly climate data (average minimum/maximum daily temperature, precipitation, fractional sunshine hours, humidity, shortwave radiation: not all of the DGVMs use all variables) from 1631 land grid cells covering the Earth's land area (excluding Antarctica). To adjust for climate model bias, all climate model outputs were taken as anomalies relative to the 1931–60 simulated mean climate and applied to an observed climatology for the same period (updated and re-gridded data from Leemans & Cramer 1991). This procedure preserved interannual variability and global sensitivity of the climate model, while simultaneously forcing the spatial pattern to be in agreement with recent observations.

For model initialization (such as the build-up of long-term soil carbon pools), a steady-state, preindustrial climate time series was created, using data from 31 years of control run GCM output, adjusted by the same bias removal method. The 31 years were repeated by the models, yielding a dataset corresponding to average mid 19th century conditions (labelled for practical reasons '1830–1860'), with the interannual variability of the GCM at low CO_2 concentration, until equilibrium, defined by no change in vegetation cover nor carbon pools during 30 years, was reached.

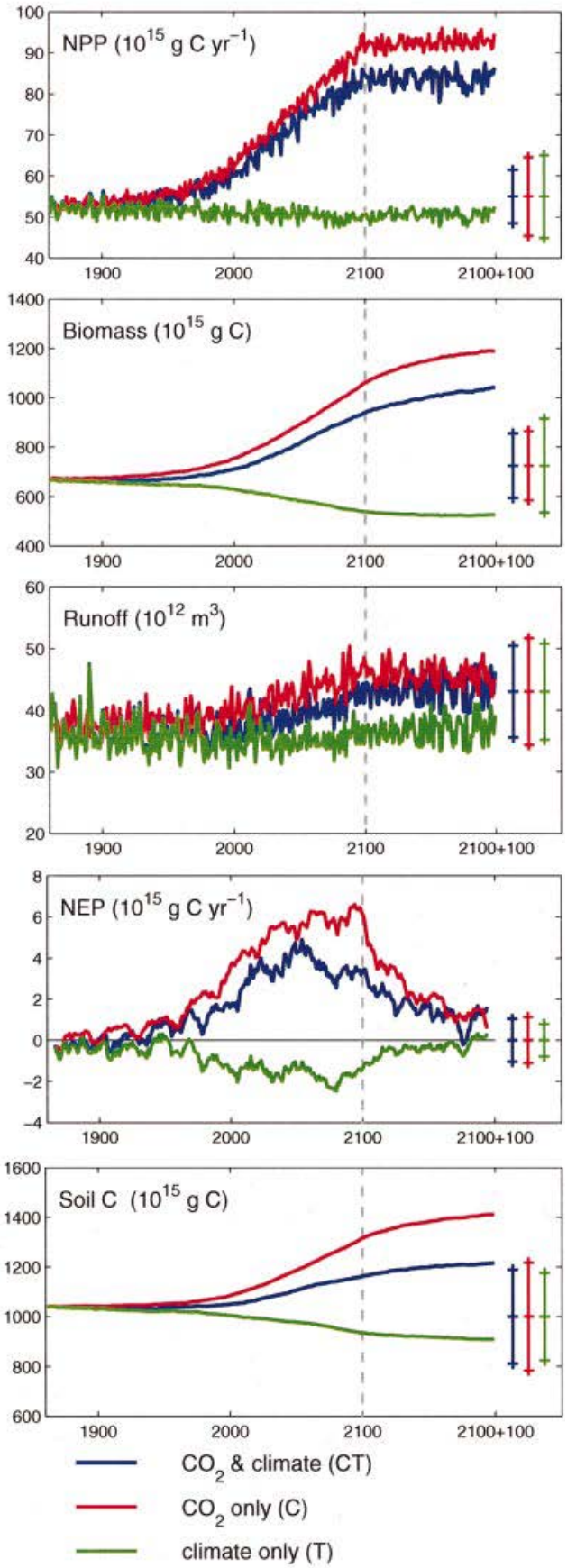
For a deliberately unrealistic 'stabilization' scenario of both CO_2 and climate after 2100, the simulated GCM years 2070–2099 were locally detrended for each pixel, and their mean value adjusted to the average of the long-term trend in the year 2100. A new 100 years time series was then created containing a randomized draw from the such modified years 2070–2099. The resulting scenario shows an abrupt levelling-off of the mean values while maintaining the interannual variability as generated by the GCM at high CO_2 concentration.

All input and output datasets for the simulations can be downloaded from a website dedicated to this study through http://www.pik-potsdam.de/data/dgvm_gcb_2000/. The site also contains links to the model development team homepages (where available) and to other relevant information.

Results

Model simulations of the present day

Model simulations of vegetation function, structure and distribution can be tested against present-day observations, providing a simultaneous assessment of the simulated climate and ecosystem response. Simulated distributions of vegetation types (Fig. 2) indicate some differences among the models, but the map of the



dominant vegetation class among models shows fair agreement ($\kappa = 0.42$, cf. Cohen 1960; Monserud & Leemans 1992) with a satellite-derived map of contemporary natural vegetation types.

Simulations are shown for historical and projected changes in global total fluxes and pools, averaged across models (Fig. 4). Simulated total net primary production (NPP) and biomass values fall within the ranges of other estimates (all of which are also at least in part model-based) at 45–60 Pg C y^{-1} (Cramer *et al*. 1999) and 500–950 Pg C, respectively (Houghton & Skole 1990; Eswaran *et al*. 1993; Schimel *et al*. 1996; Post *et al*. 1997). Model estimates (Fig. 4) of soil carbon (850–1200 Pg C) are somewhat lower than global totals derived from field measurements (Bouwman 1990; Eswaran *et al*. 1993);

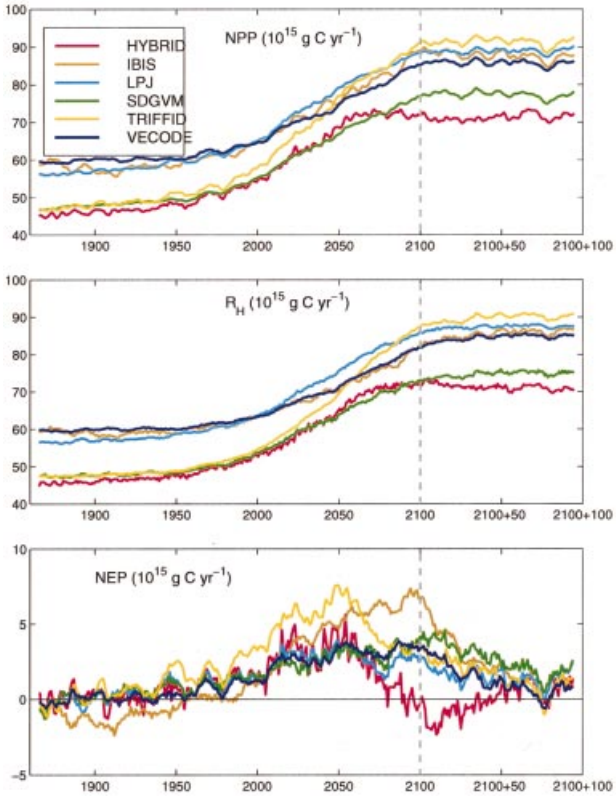


Fig. 5 Time series of simulated NEP, NPP and heterotrophic respiration (R_h) (10-y running average) from all six models, from experiment CT (both CO_2 and climate change).

Fig. 4 Time series of simulated global net primary production (NPP), net ecosystem production (NEP: 10-y running average), biomass carbon, soil carbon, and runoff for the three experiments, averaged across models (VECODE does not compute runoff). The error bars show the variation among models (time-averaged SD).

however, these measurements are relatively sparse and the totals have considerable uncertainty (Eswaran *et al*. 1993). Global totals of freshwater runoff (Fig. 4) are close (36.5×10^{15} kg y^{-1}) to the current estimate (Chahine 1992), with three of the five models (SDGVM, LPJ, IBIS) being within 10% of this value.

We derived net ecosystem production (NEP) estimates as absolute increments of total carbon stores (vegetation, litter, soil). All models show positive global NEP during recent years for experiments involving increasing CO_2 (C and CT), i.e. they indicate that the terrestrial carbon balance is not in equilibrium today (Figs 4 & 5). For the 1990s, the positive NEP in all models is substantial, caused by the increasing atmospheric CO_2 concentration (Fig. 6). In experiment C, the average NEP across all models is 2.4 Pg C y^{-1} (range 1.4–3.8) and this sink is distributed fairly evenly between the tropics and the high northern mid-and high latitudes (this is similar to the results of Kicklighter *et al*. 1999; who performed a comparable experiment based on historical climatology with a series of terrestrial biogeochemical models).

The effect of the simulated climate changes in experiment T, however, is to generate negative NEP amounting to −1.0 Pg C y^{-1} (range −0.3 to −1.9). Most models show this carbon source to be mainly in the tropics and southern hemisphere (the exception to this pattern is SDGVM, which shows a small sink in the equatorial band in experiment T). When combined in experiment CT, the effect of the climate change is to reduce the strength of the sink as found in experiment C. The average NEP in experiment CT is 1.6 Pg C y^{-1} (range 0.6–3.0), i.e. only 65% of the average NEP resulting from CO_2 effects alone. Averaged across models, the proportion of global NEP located north of 45 °N increases from 19% in experiment C to 31% in experiment CT, and this proportion increases in all models. Thus, the models agree that the contemporary carbon sink is weaker than it would be without recent climate change and that this effect is primarily a result of the effects of climate change in the tropics and mid-latitudes.

The combination of climate and CO_2 effects is not strictly additive, as can be seen by comparing experiments CT and C + T in Fig. 6. Globally and for most latitude bands, most models show greater NEP when CO_2 effects are combined with climate effects than would be expected for a linear superposition of effects. This is probably because of the increasing temperature optimum of photosynthesis at higher CO_2 concentrations and/or the mitigating effects of CO_2-induced stomatal closure on the water balance. However, there are exceptions. IBIS, in particular, shows the opposite trend (negative synergism) for the tropics and subtropics and simulates negative NEP south of 15 °N in experiment CT.

Simulated historical changes cannot be compared with individual years in the historical record of events (e.g. El Niño) because the GCM does not simulate such episodes at the same time as they occurred in reality. General trends can be compared nonetheless. Independent evidence from the atmospheric CO_2 budget (Keeling *et al*. 1995; Schimel *et al*. 1996), carbon isotopes (Ciais *et al*. 1995) and atmospheric O_2:N_2 ratios (Keeling *et al*. 1996b) supports the models' finding of a carbon sink ($\approx$ 2 Pg C y^{-1}) in unmanaged ecosystems during the 1980s and 1990s, located at both high and low latitudes (Heimann 1997; Prentice *et al*. 2000). A low-latitude component to the sink has also been inferred from small-scale field observations (Grace *et al*. 1996) but is masked in global-scale atmospheric measurements by CO_2 emissions from tropical deforestation which are apparently of similar magnitude (Melillo *et al*. 1996).

The finding that recent global warming has overall reduced the strength of the terrestrial CO_2 sink, especially in the tropics, is consistent with the observation that the CO_2 growth rate in the atmosphere is anomalously large during strong El Niño years (Braswell *et al*. 1997; Heimann 1997; Prentice *et al*. 2000). Two of the models (LPJ and SDGVM, results not shown here) have also been run with historical climate anomalies from the 1960s onward and have been shown to yield interannual variations in NEP that are negatively correlated with interannual variations in the CO_2 growth rate (Prentice *et al*. 2000), as well as good agreement between simulated NEP and NEP determined from biophysical measurements (CO_2, O_2 and stable isotopes of carbon). Such comparisons help to confirm the models' ability to simulate at least the interannual and decadal-scale components of variability in terrestrial carbon exchange.

Model projections to 2100

All of the models show an increase of the terrestrial carbon sink during the next century, driven by the continuing rise in atmospheric CO_2 concentration. In experiment C, after a century of increasing CO_2 with no change in climate, simulated average NEP has reached 6.2 Pg C y^{-1} (range 3.7–8.6 Pg C y^{-1}) with the increase occurring in the tropics and mid-latitudes as well as the northern high latitudes. However, the response of the different models to the climate change in experiment T is divergent. The average NEP across models in experiment T has become −1.7 Pg C y^{-1} (i.e. about a 70% increase in the CO_2 source). The range is large, from −3.8 to +0.2 Pg C y^{-1}. Four out of the six models show more negative NEP, the shift occurring in the north, in the northern mid-latitudes and in the tropics rather than in the southern mid-latitudes, which show no change or a

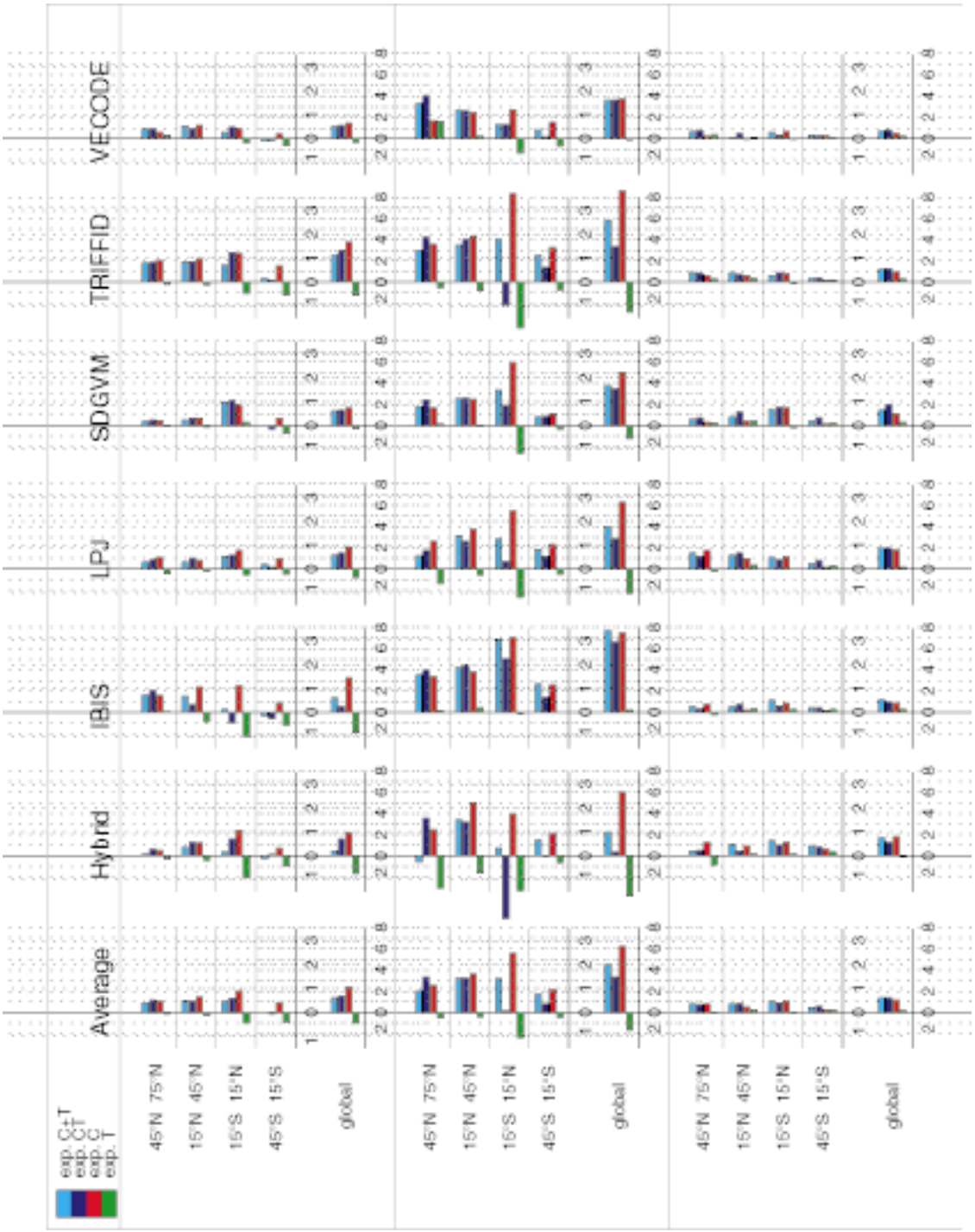


Fig. 6 Global and latitudinal simulated NEP (10-y averages) from all six models and all experiments, for three 10-y time-slices at the end of the 20th and the 21st century and after 100 y of CO_2 and climate 'stabilization'.

less negative NEP. VECODE, however, produces a substantially increased positive NEP in the north, resulting in a very small global source ($-0.1\,Pg\,C\,y^{-1}$); IBIS produces substantially more positive NEP in the tropics and mid-latitudes, resulting in a small global sink ($+0.2\,Pg\,C\,y^{-1}$). These differences reflect different responses of global NPP (not shown) to the climate change. VECODE shows a particularly strong enhancement of northern high-latitude NPP while IBIS shows an enhancement of low-latitude NPP; as a result, the trend

of global NPP is upward in these two models, whereas it is downward in the other four models. NPP, rather than R_H, is responsible for these differences in model behaviour in experiment T: the trend of R_H (not shown) is upward (tending to create a carbon source) in all of the models.

When CO_2 and climate change effects are combined in experiment CT, the range of simulated NEP values at the end of the next century is even larger than the range in experiment T. The average NEP over models is $3.4\,Pg\,C\,y^{-1}$, i.e. only about 50% of the NEP expected from CO_2 effects alone. Among models, the range is from just $0.3\,Pg\,C\,y^{-1}$ (HYBRID) to $6.6\,Pg\,C\,y^{-1}$ (IBIS). Linear superposition of climate and CO_2 effects gives a smaller range, from $2.2\,Pg\,C\,y^{-1}$ (HYBRID) to $7.7\,Pg\,C\,y^{-1}$ (IBIS). and in marked contrast to the situation for the 1990s, CO_2 and climate change together consistently produce a *lower* NEP than would be expected from linear superposition. The latitudinal breakdown of this effect (Fig. 6) shows that this change is consistently associated with tropical and southern mid-latitude ecosystems. Northern ecosystems continue to show positive synergism while tropical ecosystems in particular show strong negative synergism. In other words, climate change in these simulations has by 2100 substantially weakened the ability of tropical and southern mid-latitude ecosystems to store carbon in response to rising atmospheric CO_2.

The comparison of modelled trends in NPP and R_H in experiment CT (Fig. 5) is dominated by the effect of rising CO_2 on both. NPP increases in all model simulations, although the increase is noticeably steeper in TRIFFID than in the other models. It is also clear from Fig. 5 that NPP in HYBRID stops increasing at about 2050 and remains approximately constant thereafter. The overall trend in R_H is dominated by the increase in the size of the respiring pool brought about by increasing NPP, and therefore mirrors the NPP changes with a lag on the order of 20–30 y, which is not easily discernible from a visual comparison of the time trends in NPP and R_H.

The time-course of NEP (which strongly depends on this lag; cf. Kicklighter *et al*. 1999) tells a more subtle story. At present, on average over several decades, all the models show increasing NEP, but the rate of increase starts to level off in *all* of these models by about 2030. By 2050, all models but IBIS are showing declining NEP and even in IBIS the curve of NEP with time has become virtually flat. In other words, the combination of mechanisms that may be acting to reduce the global carbon sequestration potential of ecosystems (including 'saturation' of the CO_2 response mechanism, increasing R_H in response to warming, and according to some models reduced NPP in the tropics) has already by 2050 produced a strong flattening of the NEP curve and in some models (notably HYBRID) has initiated a steep decline in NEP.

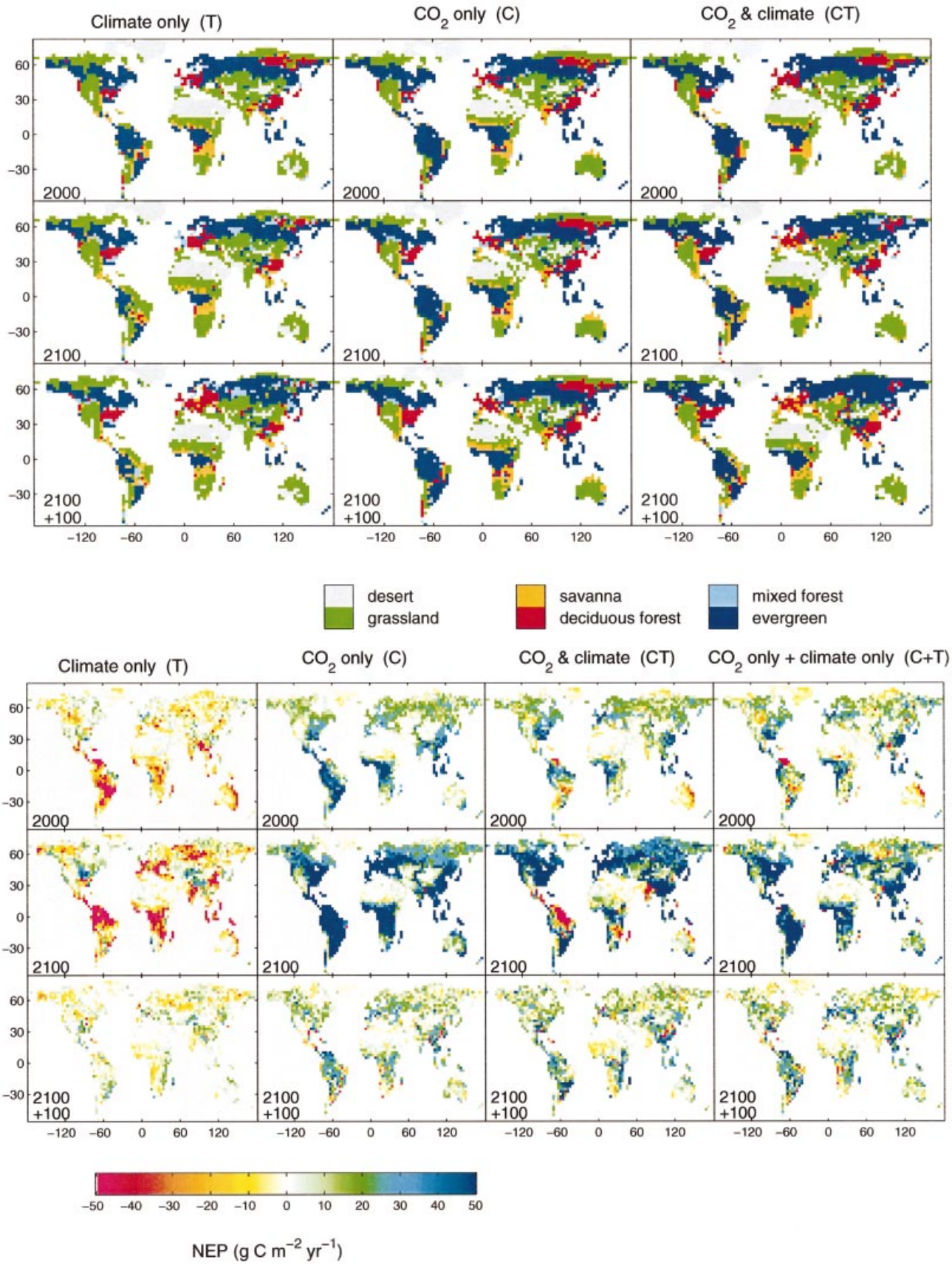
These NEP trends, if they are realistic, would have implications for the projected future contribution of terrestrial ecosystems to the global atmospheric carbon budget. In experiment C the models allow the terrestrial biosphere to take up more than 35% (range 22–57%) of the projected anthropogenic carbon emissions between 1991 and 2100 (1530 Pg C, Wigley & Raper 1992). However, the increase in NEP levels off fairly sharply around 2030, even in this experiment, with no change in climate (Fig. 4). In experiment T, by contrast, the models simulate a climate-induced release of carbon, corresponding to ≈ 10% (range 3–23%) of the additional CO_2 emissions. Average model results for experiment CT show an uptake of ≈ 23% (range 17–35%) of projected emissions, i.e. the CO_2 effect dominates but the resulting sink is substantially weakened due to the changing climate.

CO_2-induced increases in water-use efficiency and hence reduced transpiration translate into increased runoff (Fig. 4) by all models except one (−3% −+47% from 1990 to 2100 in experiment C, +1% −+45% in experiment CT). Climate change only has a small impact on runoff (−1% −+9% in experiment T). These figures can be compared to the 4% increase in precipitation over land predicted by HadCM2 SUL. Without vegetation change effects, a water resources model driven by HadCM2 SUL produced a 6.5% increase in global runoff (N. Arnell, unpubl. data). The simulated changes in precipitation are far from uniform and some areas, such as northern Amazonia receive marked reductions in precipitation that reduce vegetation from a forest to a grassland (Fig. 7).

The effects of CO_2 alone (experiment C) on vegetation structure are relatively minor, with some expansion of forests into savanna and grassland into arid regions of

Fig. 7 (top right) Simulated vegetation distribution (dominant class as in Fig. 2) from the three experiments at the end of the 20th and the 21st century and after 100 years of CO_2 and climate 'stabilization'.

Fig. 8 (bottom right) Model average NEP at 2000, 2100 and the 'stabilization period' 2100 + 100 from the three experiments (mean of last 10 years in each century). The final column shows the sum of NEP from the climate-only and CO_2-only experiments.


Climate only (T)
CO2 only (C)
CO2 & climate (CT)
2000
2100
2100 +100
60
30
0
−30
−120
−60
0
60
120
desert
grassland
savanna
deciduous forest
mixed forest
evergreen
Climate only (T)
CO2 only (C)
CO2 & climate (CT)
CO2 only + climate only (C+T)
−50
−40
−30
−20
−10
0
10
20
30
40
50
NEP (g C m−2 yr−1)

the tropics (Fig. 7). Larger changes in vegetation distribution and structure occur in response to warming (e.g. the extension of forest at high latitudes) and especially in response to regional precipitation shifts. Changes in climate alone (experiment T) have large, and correlated, impacts on vegetation distribution (Fig. 7) and NEP (Fig. 8). Inspection of these maps suggests an explanation for the changes in NEP previously noted. Some regions of Africa, America and SE Asia, in particular, become carbon sources in experiment T because simulated regional drought causes forest dieback and reduced NPP. In the combined experiment CT, the climate-induced expansion of (initially deciduous) forests in Siberia allows an enhanced response of NEP to increasing CO_2 during the next century. The expansion of deciduous forest in Europe is accompanied by reduced precipitation and decreased NEP, but this is opposed by North America, where deciduous forest expansion is accompanied by increased precipitation and increased NEP (VEMAP Members 1995). In those tropical regions affected by drought in the simulated climate, the areas where forest dieback is simulated suffer not only from a loss of carbon but also a change in vegetation composition (towards C4-dominated grassland), which further reduces the potential of these areas to respond to increasing CO_2.

The immediate 'stabilization' of climate and atmospheric CO_2 concentrations in 2100 (Fig. 2) is intentionally unrealistic and designed to probe the extent to which ecosystem processes will be out of equilibrium with climate after more than a century of global warming. Global NEP approaches zero in all experiments by 2100 + 100, implying that the global average of terrestrial carbon fluxes are approaching equilibrium, but changes in vegetation structure are still ongoing – especially the extension of evergreen forests in high latitudes (Canada and Siberia). Persistent regional patterns of carbon source and sink activity (Figs 6 & 8) reflect these continuing changes.

Discussion and conclusions

Robust results of these model experiments include the simulation of a contemporary terrestrial carbon sink of approximately the right magnitude to explain recent geophysical observations of terrestrial carbon uptake (Ciais *et al*. 1995; Keeling *et al*. 1995; Keeling *et al*. 1996a; Keeling *et al*. 1996b; Fung *et al*. 1997), while indicating that this sink cannot be assumed to be able to increase indefinitely. In addition to the expected 'saturation' of the direct CO_2 physiological fertilizing effect at high CO_2 concentrations (Cao & Woodward 1998), the majority of the models shows a progressive erosion of the carbon sink by climatic change after 2050, in part a result of increased heterotrophic respiration, in part a result of regional precipitation reductions which under the particular climate change scenario we used lead to the replacement of some tropical forest areas by grasslands, and a reduction in tropical NEP. Forests are also vulnerable to increasing population pressure in so far as this leads to permanent deforestation, so a complete picture of ecosystem changes will have to take into account the spatial relationships between climate effects and land-use patterns.

We emphasize that the regional details of these simulations are not to be taken as predictions. Regional precipitation patterns are among the least consistent and reliable aspects of current climate models (Hulme *et al*. 1998). Nevertheless, our results (Figs 6 & 8) point to the key importance of regional climatic change both for the direct impacts on terrestrial ecosystems and for the hydrological and carbon cycles in which terrestrial ecosystems are enmeshed. Long-term calculations of CO_2 stabilization options (Wigley *et al*. 1996; Wigley 1997) as well as projections of ecological and hydrological impacts of climate change (Watson *et al*. 1996) should therefore be revisited with the help of models that include the dynamic evolution of vegetation and its influence on the global carbon and water cycles. Meanwhile, attention must be paid to improved validation methods (Cramer *et al*. 1999; Scurlock *et al*. 1999) to discriminate among the divergent responses of current models, particularly as regards the magnitude of response of NPP to climate change in northern vs. tropical forests and the sensitivity of tropical ecosystem function to regional precipitation changes.

Differences between models are noteworthy and not easily related to model complexity or specific process formulations—these differences are being investigated further. Reduced-complexity models, such as TRIFFID and VECODE, offer the advantage of high computational efficiency against a more limited possibility of deriving knowledge for particular processes. They are therefore highly suitable for long-term integration and for the study of feedbacks in coupled Earth System models, while more complex models such as SDGVM, LPJ, HYBRID and IBIS allow for more direct studies of ecophysiological processes and their implications at the global scale.

Ultimately, the development of DGVMs is expected to lead to better tools for the assessment of impacts on multiple ecosystem services beyond carbon storage, such as water resources, conservation values and forest productivity. Many assessments, such as the reports of the IPCC, indicate that these services might be vulnerable if they were confronted with the changes expected in underlying ecosystem processes.

Acknowledgements

We are grateful for funding of this research by the DETR, EPRI, EU, NASA, NERC UK and NSF. The work by PMC and RAB, and that for HadCM2, forms part of the UK DETR Climate Prediction Programme. The work is part of the IGBP core project GCTE. We also gratefully acknowledge technical support by Karsten Kramer and Dietmar Gibietz-Rheinbay, Potsdam Institute for Climate Impact Research.

References

Betts RA, Cox PM, Lee SE, Woodward FI (1997) Contrasting physiological and structural vegetation feedbacks in climate change simulations. *Nature,* **387,** 796–799.

Bouwman AF (ed.) (1990) *Soils and the greenhouse effect: the present status and future trends concerning the effect of soils and their cover on the fluxes of greenhouse gases, the Surface Energy Balance and the Water Balance.* Wiley, Chichester.

Braswell BH, Schimel DS, Linder E, Moore B III (1997) The response of global terrestrial ecosystems to interannual temperature variability. *Science*, **278** (5339)**,** 870–872.

Brovkin V, Ganopolski A, Svirezhev Y (1997) A continuous climate-vegetation classification for use in climate-biosphere studies. *Ecological Modelling*, **101,** 251–261.

Cao M, Woodward FI (1998) Dynamic responses of terrestrial ecosystem carbon cycling to global climate change. *Nature,* **393,** 249–252.

Chahine MT (1992) The hydrological cycle and its influence on climate. *Nature*, **359,** 373–380.

Ciais P, Tans PP, Trolier M, White JWC, Francey RJ (1995) A large northern hemisphere terrestrial CO_2 sink indicated by the $^{13}C/^{12}C$ ratio of atmospheric CO_2. *Science*, **269** (5227)**,** 1098–1102.

Clark JS, Fastie C, Hurtt G *et al*. (1998) Reid's paradox of rapid plant migration: dispersal theory and interpretation of paleoecological records. *Bioscience*, **48,** 13–24.

Cohen J (1960) A coefficient of agreement for nominal scales. *Educational and Psychological Measurements*, **20,** 37–46.

Collatz GJ, Ball JT, Grivet C, Berry JA (1991) Physiological and environmental regulation of stomatal conductance, photosynthesis and transpiration: a model that includes a laminar boundary layer. *Agricultural and Forest Meteorology*, **54,** 107–136.

Collatz GJ, Ribas-Carbo M, Berry JA (1992) A coupled photosynthesis – stomatal conductance model for leaves of C4 plants. *Australian Journal of Plant Physiology*, **19,** 519–538.

Comins HN, McMurtrie RE (1993) Long-term response of nutrient-limited forests to CO_2 enrichment – equilibrium behavior of plant-soil models. *Ecological Applications*, **3** (4)**,** 666–681.

Cox PM, Huntingford C, Harding RJ (1998) A canopy conductance and photosynthesis model for use in a GCM land surface scheme. *Journal of Hydrology*, **212–213,** 79–94.

Cramer W (1996) Modeling the possible impact of climate change on broad-scale vegetation structure: examples from northern Europe. In: *Global Change and Arctic Terrestrial Ecosystems* (eds Oechel WC *et al.*), pp. 312–329. Springer, New York.

Cramer W (1997) Using plant functional types in a global vegetation model. In: *Plant Functional Types: Their Relevance to Ecosystem Properties and Global Change* (eds Smith TM *et al.*), pp. 271–288. Cambridge University Press, Cambridge.

Cramer W, Kicklighter DW, Bondeau A *et al*. (1999) Comparing global models of terrestrial net primary productivity (NPP): Overview and key results. *Global Change Biology*, **5** (Supplement 1)**,** 1–15.

Dixon RK, Brown S, Houghton RA, Solomon AM, Trexler MC, Wisniewski J (1994) Carbon pools and flux of global forest ecosystems. *Science*, **263** (5144)**,** 185–190.

Eswaran H, van der Berg E, Reich P (1993) Organic carbon in soils of the world. *Soil Science Society of America Journal*, **57,** 192–194.

Fan S, Gloor M, Mahlman J, Pacala S, Sarmiento J, Takahashi T, Tans P (1998) A large terrestrial carbon sink in North America implied by atmospheric and oceanic carbon dioxide data and models. *Science*, **282,** 442–446.

Farquhar GD, von Caemmerer S, Berry JA (1980) A biochemical model of photosynthetic CO_2 assimilation in leaves of C_3 species. *Planta*, **149,** 78–90.

Foley JA, Prentice IC, Ramankutty N, Levis S, Pollard D, Sitch S, Haxeltine A (1996) An integrated biosphere model of land surface processes, terrestrial carbon balance, and vegetation dynamics. *Global Biogeochemical Cycles*, **10** (4)**,** 603–628.

Friend AD (1995) PGEN – an integrated model of leaf photosynthesis, transpiration, and conductance. *Ecological Modelling*, **77** (2–3)**,** 233–255.

Friend AD, Stevens AK, Knox RG, Cannell MGR (1997) A process-based, terrestrial biosphere model of ecosystem dynamics (Hybrid v3.0). *Ecological Modelling*, **95,** 249–287.

Fung I, Field CB, Berry JA *et al*. (1997) Carbon 13 exchanges between the atmosphere and biosphere. *Global Biogeochemical Cycles*, **11,** 507–533.

Ganopolski A, Kubatzki C, Claussen M, Brovkin V, Petoukhov V (1998) The influence of vegetation-atmosphere–ocean interaction on climate during the mid-Holocene. *Science*, **280,** 1916–1919.

Grace J, Malhi Y, Lloyd J *et al.* (1996) The use of eddy covariance to infer the net carbon dioxide uptake of Brazilian rain forest. *Global Change Biology*, **2** (3)**,** 209–217.

Haxeltine A, Prentice IC (1996a) BIOME3: an equilibrium biosphere model based on ecophysiological constraints, resource availability and competition among plant functional types. *Global Biogeochemical Cycles*, **10** (4)**,** 693–709.

Haxeltine A, Prentice IC (1996b) A general model for the light-use efficiency of primary production. *Functional Ecology*, **10** (5)**,** 551–561.

Heimann M (1997) A review of the contemporary global carbon cycle and as seen a century ago by Arrhenius and Högbom. *Ambio*, **26** (1)**,** 17–24.

Heimann M, Kaminski T (1999) Inverse modelling approaches to infer surface trace gas fluxes from observed atmospheric mixing ratios. In: *Approaches to Scaling Trace Gas Fluxes in Ecosystems* (ed. Bouwman AF). Elsevier Science, Amsterdam.

Houghton JT, Callander BA, Varney SK (eds) (1992). *Climate Change 1992 – the Supplementary Report to the IPCC Scientific Assessment*. Cambridge University Press, Cambridge.

Houghton RA, Hackler JL, Lawrence KT (1999) The U.S. carbon budget: contributions from land-use change. *Science*, **285,** 574–578.

Houghton RA, Skole DL (1990) Carbon – Transformations of the Global Environment. In: *The Earth as Transformed by Human*

Action – Global and Regional Changes in the Biosphere Over the Past 300 Years (eds Turner BL *et al.*), pp. 393–408. Cambridge University Press, Cambridge.

Hulme M, Osborn TJ, Johns TC (1998) Precipitation sensitivity to global warming: comparison of observations with HadCM2 simulations. *Geophysical Research Letters*, **25,** 3379–3382.

IGBP Terrestrial Carbon Working Group (1998) The terrestrial carbon cycle: implications for the Kyoto Protocol. *Science*, **280,** 1393–1394.

Jarvis P (1976) The interpretation of the variations in leaf water potential and stomatal conductance found in canopies in the field. *Philosophical Transactions of the Royal Society of London Series B*, **273,** 593–610.

Johns TC, Carnell RE, Crossley JF *et al.* (1997) The second Hadley Centre coupled ocean-atmosphere GCM: model description, spinup and validation. *Climate Dynamics*, **13,** 103–134.

Jones PD (1994) Hemispheric surface air temperature variations: a reanalysis and an update to 1993. *Journal of Climate*, **7,** 1794–1802.

Kattenberg A, Giorgi F, Grassl H *et al.* (1996) Climate Models – Projections of Future Climate. In: *Climate Change 1995 – the Science of Climate Change* (eds Houghton JT *et al.*), pp. 285–357. Cambridge University Press, Cambridge.

Keeling CD, Chin JFS, Whorf TP (1996a) Increased activity of northern vegetation inferred from atmospheric CO_2 measurements. *Nature*, **382** (6587)**,** 146–148.

Keeling RF, Piper SC, Heimann M (1996b) Global and hemispheric CO_2 sinks deduced from changes in atmospheric O_2 concentration. *Nature,* **381,** 218–221.

Keeling CD, Whorf TP, Wahlen M, Van der Plicht J (1995) Interannual extremes in the rate of rise of atmospheric carbon dioxide since 1980. *Nature*, **375** (6533)**,** 666–670.

Kicklighter DW, Bruno M, Dönges S *et al.* (1999) A first order analysis of the potential of CO_2 fertilization to affect the global carbon budget: a comparison of four terrestrial biosphere models. *Tellus*, **51B,** 343–366.

King AW, Post WM, Wullschleger SD (1997) The potential response of terrestrial carbon storage to changes in climate and atmospheric CO_2. *Climatic Change*, **35,** 199–227.

Leemans R, Cramer W (1991) *The IIASA database for mean monthly values of temperature, precipitation and cloudiness of a global terrestrial grid.* International Institute for Applied Systems Analysis (IIASA). RR-91–18.

Leuning R (1995) A critical appraisal of a combined stomatal-photosynthesis model for C_3 plants. *Plant, Cell and Environment*, **18** (4)**,** 339–355.

Lloyd J, Farquhar GD (1996) The CO_2 dependence of photosynthesis, plant growth responses to elevated atmospheric CO_2 concentrations and their interaction with soil nutrient status.1. General principles and forest ecosystems. *Functional Ecology*, **10** (1)**,** 4–32.

Lloyd J, Taylor JA (1994) On the temperature dependence of soil respiration. *Functional Ecology*, **8** (3)**,** 315–323.

Loveland TR, Belward AS (1997) The IGBP-DIS global 1km land cover data set, DISCover: first results. *International Journal of Remote Sensing*, **18,** 3289–3295.

McGuire AD, Melillo JM, Joyce LA *et al.* (1992) Interactions between carbon and nitrogen dynamics in estimating net primary productivity for potential vegetation in North America. *Global Biogeochemical Cycles*, **6** (2)**,** 101–124.

Melillo JM, Prentice IC, Farquhar GD, Schulze E-D, Sala OE (1996) Terrestrial Biotic Responses to Environmental Change and Feedbacks to Climate. In: *Climate Change 1995 – the Science of Climate Change* (eds Houghton JT *et al.*), pp. 445–481. Cambridge University Press, Cambridge.

Mitchell JFB, Johns TC, Gregory JM, Tett SFB (1995) Climate response to increasing levels of greenhouse gases and sulphate aerosols. *Nature*, **376,** 501–504.

Monserud RA, Leemans R (1992) Comparing global vegetation maps with the Kappa statistic. *Ecological Modelling*, **62,** 275–293.

Monteith JL (1981) Evaporation and environment. In: *The State and Movement of Water in Living Organisms* (ed. Fogg CE), pp. 205–234.

Monteith JL (1995) Accommodation between transpiring vegetation and the convective boundary layer. *Journal of Hydrology*, **166** (3–4)**,** 251–263.

Monteith JL, Unsworth MH (1990) *Principles of Environmental Physics*. Edward Arnold, London.

Nadelhoffer KJ, Emmett BA, Gundersen P *et al.* (1999) Nitrogen makes a minor contribution to carbon sequestration in temperate forests. *Nature*, **398,** 145–148.

Neilson RP (1993) Vegetation redistribution: a possible biosphere source of CO_2 during climatic change. *Water, Air and Soil Pollution*, **70** (1–4)**,** 659–673.

Neilson RP, Prentice IC, Smith B, Kittel T, Viner D (1998) Simulated changes in vegetation distribution under global warming. In: *The Regional Impacts of Climate Change* (eds Watson RT *et al.*), pp. 439–456. Cambridge University Press, Cambridge, UK.

Parton WJ, Scurlock JMO, Ojima DS *et al.* (1993) Observations and modeling of biomass and soil organic matter dynamics for the grassland biome worldwide. *Global Biogeochemical Cycles*, **7** (4)**,** 785–809.

Pitelka LF, Plant Migration Workshop Group (1997) Plant migration and climate change. *American Scientist*, **85,** 464–473.

Pollard D, Thompson SL (1995) Use of a land-surface transfer scheme (LSX) in a global climate model: The response to doubling stomatal resistance. *Global and Planetary Change*, **10,** 129–161.

Post WM, King AW, Wullschleger SD (1997) Historical variations in terrestrial biospheric carbon storage. *Global Biogeochemical Cycles*, **11** (1)**,** 99–110.

Prentice IC, Heimann M, Sitch S (2000) The carbon balance of the terrestrial biosphere: ecosystem models and atmospheric observations. *Ecological Applications*, **10** (6), 1553–1573.

Prentice IC, Webb RS, Ter-Mikhaelian MT *et al.* (1989). *Developing a Global Vegetation Dynamics Model: Results of an IIASA Summer Workshop.* International Institute for Applied Systems Analysis, Laxenburg, Austria. RR-89-7.

Rayner PJ, Enting IG, Francey RJ, Langenfelds R (1999) Reconstructing the recent carbon cycle from atmospheric CO_2, $d^{13}C$ and O_2/N_2 observations. *Tellus*, **51B,** 668–678.

Schimel DS (1998) The carbon equation. *Nature*, **393,** 208–209.

Schimel D, Alves D, Enting I *et al.* (1996) Radiative Forcing of Climate Change. In: *Climate Change 1995 – the Science of Climate Change* (eds Houghton JT *et al.*), pp. 65–131. Cambridge University Press, Cambridge.

Scurlock JMO, Cramer W, Olson RJ, Parton WJ, Prince SD (1999) Terrestrial NPP: Toward a consistent data set for global model evaluation. *Ecological Applications*, **9** (3)**,** 913–919.

Sellers PJ (1985) Canopy reflectance, photosynthesis and

transpiration. *International Journal of Remote Sensing*, **6** (8), 1335–1372.

Sellers PJ, Berry JA, Collatz GJ, Field CB, Hall FG (1992) Canopy reflectance, photosynthesis and transpiration. III. A reanalysis using improved leaf models and a new canopy integration scheme. *Remote Sensing of Environment*, **42,** 187–216.

Sellers PJ, Bounoua L, Collatz GJ *et al*. (1996) Comparison of radiative and physiological effects of doubled atmospheric CO_2 on climate. *Science*, **271** (5254), 1402–1406.

Sitch S (2000) *The role of vegetation dynamics in the control of atmospheric CO_2 content*. PhD thesis, Lund University.

Smith TM, Shugart HH (1993) The transient response of terrestrial carbon storage to a perturbed climate. *Nature*, **361,** 523–526.

Steffen WL, Walker BH, Ingram JSI, Koch GW (1992) *Global Change and Terrestrial Ecosystems: The Operational Plan*. International Geosphere-Biosphere Programme.

Stewart JB (1988) Modelling surface conductance of pine forest. *Agricultural and Forest Meteorology*, **43,** 19–35.

Tett SFB, Johns TC, Mitchell JFB (1997) Global and regional variability in a coupled AOGCM. *Climate Dynamics*, **13,** 303–323.

United Nations Framework Convention on Climate Change (1997) *Kyoto Protocol to the United Nations Framework Convention on Climate Change*, vol. 24. UN, Geneva.

VEMAP Members (1995) Vegetation/ecosystem modelling and analysis project: Comparing biogeography and biogeochemistry models in a continental-scale study of terrestrial ecosystem responses to climate change and CO_2 doubling. *Global Biogeochemical Cycles*, **9** (4), 407–437.

Watson RT, Zinyowera MC, Moss RH (eds) (1996) Climate Change 1995: Impacts, Adaptations, and Mitigation: Scientific-Technical Analyses. In: *Contribution of Working Group II to the Second Assessment Report of the Intergovernmental Panel on Climate Change*. Cambridge University Press, Cambridge.

Watson RT, Zinyowera MC, Moss RH (eds) (1998). *The Regional Impacts of Climate Change*. Cambridge University Press, Cambridge.

Wigley TML (1997) Implications of recent CO_2 emission-limitation proposals for stabilization of atmospheric concentrations. *Nature*, **390,** 267–270.

Wigley TML, Raper SCB (1992) Implications for climate and sea level of revised IPCC emissions scenarios. *Nature*, **357,** 293–300.

Wigley TML, Holt T, Raper SCB (1991) *STUGE User's Manual*. Climatic Research Unit, University of East Anglia, Norwich.

Wigley TML, Richels R, Edmonds JA (1996) Economic and environmental choices in the stabilization of atmospheric CO_2 concentrations. *Nature*, **379,** 240–243.

Woodward FI, Cramer W (1996) Plant functional types and climatic changes – Introduction. *Journal of Vegetation Science*, **7** (3), 306–308.

Woodward FI, Lomas MR, Betts RA (1998) Vegetation-climate feedbacks in a greenhouse world. *Philosophical Transactions of the Royal Society of London Series B*, **353,** 29–38.

Woodward FI, Lomas MR, Lee SE (in press) Predicting the future production and distribution of global terrestrial vegetation. In: *Terrestrial Global Productivity* (eds Roy J *et al.*), pp. Academic Press.